NISQ-era QFT

N. Klco, E. F. Dumitrescu, A. J. McCaskey,
T. D. Morris, R. C. Pooser, M. Sanz, E. Solano,
P. Lougovski, M. J. Savage

arXiv: 1803.03326

This work is supported by the US department of Energy, Office of Science, Office of Advanced Scientific Computing Research (ASCR) quantum algorithm teams program under field work proposal number ERKJ333

[6] arXiv: 1808.10378
N. Klco and M. J. Savage

Scalar $\lambda\phi^4$

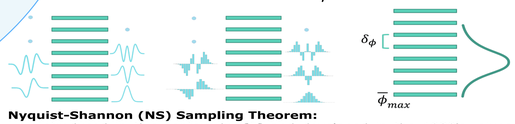

Nyquist-Shannon (NS) Sampling Theorem:

Introduced in this context by [5] and developed in the 1930's, gives guidance for digitizing continuous signals (from audio recordings to wavefunctions) when the signal has finite frequency bandwidth (as is the case for the conjugate momentum of a latticized scalar field). After reaching the NS saturation point, the structure of momentum space is captured and the description is exponentially converged.

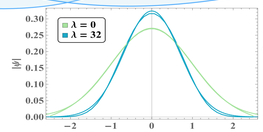

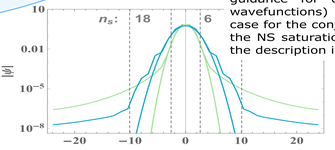

Choosing a Basis:

In order to give structure to the qubit register representing the field at a given site, any basis may be chosen. Three nice choices are: JLP [1] using the eigenstates of the field operator, MSAH [5] digitizing harmonic oscillator wavefunctions into eigenstates of the field operator and [6] using exact harmonic oscillator wavefunctions. JLP allows the field operator to be written as a sum of single qubit operators (leading to low-depth, low-entanglement circuits), while the use of harmonic oscillator bases allows a description of localized wavefunctions with fewer basis states.

Jordan-Lee-Preskill Basis:

$$e^{-i\hat{H}_3 t} = \lim_{M\to\infty} \left(\Phi_3\left(\tfrac{t}{2M}\tfrac{4}{49}\bar{\phi}^2_{max}\right) \; QFT_{sym} \left(\tfrac{x_{min}\bar{\phi}_{max}}{\bar{\phi}^2_{max}} \tfrac{p_{max}}{t}\right) \varepsilon_\Phi \; QFT^{-1}_{sym} \right)^M$$

0+1 Self-Interacting Scalar

Tuning Plots:

Given a number of qubits, it is important to construct and a basis to accurately describe the low-energy subspace, maximizing the physics captured with available quantum resources. A well-tuned basis places the computation at the NS saturation point. Left of this point, exponential convergence is achieved in the number of qubits. Right of this point, conjugate momentum space is undersampled and precision degrades. Tuning plots for the JLP and Harmonic Oscillator bases are shown at right for an interacting 0+1 dimensional scalar field. For such a localized wavefuncton, the HO basis provides higher precision per qubit.

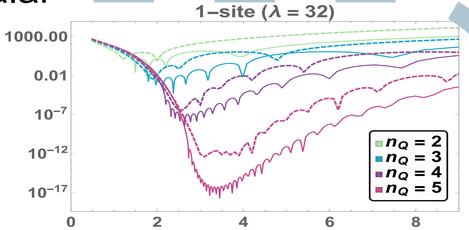

Precision, Improvement and Noise:

To implement the conjugate momentum term, one option is to retain field-space locality with a nearest neighbor operator. This choice introduces polynomial errors in the field digitization, destroying the exponential precision allowed by the NS sampling theorem (green points at left). As is done with the Symanzik action in Lattice QCD, the polynomial errors in the digitization can be order-by-order suppressed by adding higher-order operators to the Hamiltonian (blue points at left). In Quantum computing, it is possible to fourier transform to conjugate momentum space where the Pi operator is diagonal, allowing improvement to all orders. With quantum noise, the NS saturation point should be tuned to match the expected precision of quantum hardware.

$1.4\sqrt{\frac{2^{n_Q}}{\omega_\phi}}$ or $\bar{\phi}_{max}$

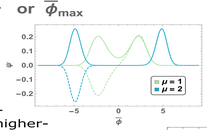

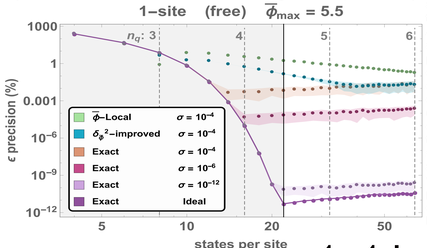

Harmonic Oscillator Basis:

$$e^{-i(H_{basis}+\delta H_{\omega_\phi})t} = \lim_{M\to\infty}$$

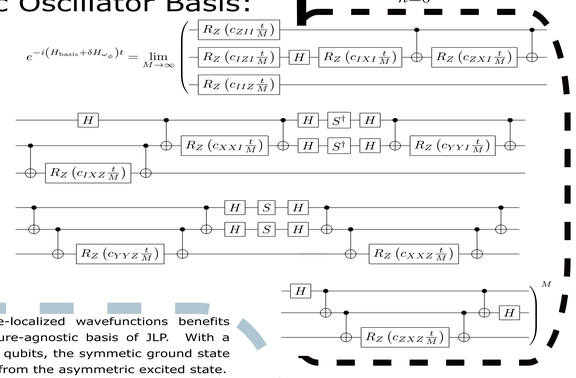

Representing de-localized wavefunctions benefits from the structure-agnostic basis of JLP. With a tuned basis of 6 qubits, the symmetic ground state is distinguished from the asymmetric excited state.

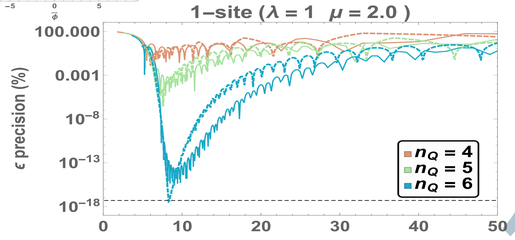

1+1 Lattice and Circuitry

Basis	n_Q	2-body	3-body	4-body	5-body	6-body	7-body	8-body	9-body	10-body	11-body	12-body	CNOT
JLP	2	4											8
	3	9											18
	4	16											32
	5	25											50
	6	36											72
	n_Q	n_Q^2											$2n_Q^2$
HO	2	1	6	9									80
	3	1	8	30	56	49							1,152
	4	1	10	47	140	271	330	225					11,264
	5	1	12	68	244	630	1204	1668	1612	961			89,600
	6	1	14	93	392	1186	2772	5154	7560	8541	7182	3969	626,688

Implementation of the Gradient Operator:

On the right, the quantum resources for representation of the scalar field at a single site are quantified. In order to connect the qubit registers to build lattices in higher spatial dimensions, we quantify the cost of a nearest neighbor decomposition of the gradient operator in field space (table above). As was the case in the single site, the JLP basis requires only 2-qubit interactions between the two site registers while the HO basis requires entangling interactions between all qubits within the pair of site registers. The resulting number of CNOTs naively required to interact two 6-qubit site registers differs by a factor of ~8700. As was the case for the conjugate momentum operator, the QFT could be used to remove polynomial errors in the lattice spacing. However, the proposed retention of locality for the gradient avoids both the maximum size of entangling operators and the computation time for trotterized time evolution from growing with the size of the lattice---a naturally-motivated and desrable scaling.

$2.9\sqrt{\frac{2^{n_Q}}{\omega_\phi}}$ or $\bar{\phi}_{max}$

The field operator in the JLP basis can be written as a sum of single-qubit operators. As a result, the qubit interactions for each spatial site are limited to two-body operators (QFT and mass term) and four-body operators (fourth-order self-interaction) for the Trotterized time evolution. Pauli decomposition of the HO propagator contains interactions between all qubits in the site register, causing the number of 2-qubit entangling operators to grow more rapidly in the HO basis.

Basis	n_Q	0-body	1-body	2-body	3-body	4-body	5-body	6-body	CNOTs
JLP	2	1	8	2					8
	3	1	14	6					24
	4	1	20	12		1			54
	5	1	26	20		5			110
	6	1	32	30		15			210
JLP	n_Q	1	$4n_Q-6$	$2*\binom{n_Q}{2}$		$\binom{n_Q}{4}$			$8\binom{n_Q}{2}+6\binom{n_Q}{4}$
HO	2	1	3	1					4
	3	1	5	9	4				34
	4	1	6	16	18	10			164
	5	1	7	22	32	44	22		612
	6	1	8	29	44	84	98	46	1982

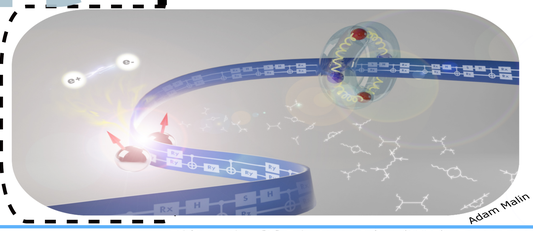

Bibliography: [1] Jordan, Stephen P., Lee, Keith S. M. & Preskill, John (2012). Quantum Algorithms for Quantum Field Theories. Science, 336, 1130-1133.
[2] Jordan, Stephen P., Lee, Keith S. M. & Preskill, John (2011). Quantum Computation of Scattering in Scalar Quantum Field Theories. Quant. Inf. Comput.14,1014 (2014).
[3] Somma, Rolando D. (2016). Quantum Simulations of One DImensional Quantum Systems. Quantum Information and Computation, Vol. 16, No. 13&14 (2016) 1125–1168.
[4] Yeter-Aydeniz, Kubra & Siopsis, George (2018). Quantum computation of scattering amplitudes in scalar quantum electrodynamics. Phys. Rev. D, 97, 036004.
[5] Alexandru Macridin, Panagiotis Spentzouris, James Amundson, Roni Harnik (2018). Electron-Phonon Systems on a Universal Quantum Computer. ArXiv: 1802:07347v2

1+1 Electrodynamics

The Schwinger Model:

Quantum electrodynamics in one spatial dimension shares many features with QCD such as confinement (along with a screening vacuum) and spontaneous breaking of chiral symmetry. When this theory is latticized with staggered fermions and transformed to spin degrees of freedom using the Jordan-Wigner transformation, the Hamiltonian describing the system may be written as below. The kinetic (hopping) term contains raising and lowering operators, modifying the value of the electric field on the link (which is naturally quantized in one dimension and here truncated at field values $\mp$ 1) while creating or annihilating an electron-positron pair at the associated sites on either side. In this model, there is only one dynamical link---all others can be contstrained by Gauss's law and the distribution of the fermion content. Rather than integrating out these degrees of freedom and producing non-local interactions, we choose to work with physical, symmetry-projected configurations of the lattice. As a result, inevitable errors occurring in today's noisy quantum devices are incapable of populating states outside of the correct dynamical Hilbert space.

$$\hat{H} = x \sum_{n=0}^{N_{fs}-1} \left(\sigma_n^+ L_n^- \sigma_{n+1}^- + \sigma_{n+1}^+ L_n^+ \sigma_n^-\right) + \sum_{n=0}^{N_{fs}-1} \left(l_n^2 + \frac{\mu}{2}(-)^n \sigma_n^z\right)$$

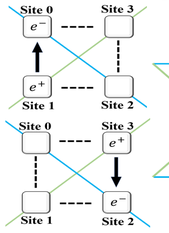

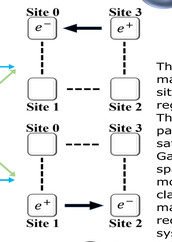

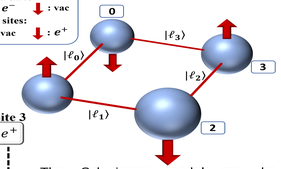

The Schwinger model can be mapped to qubits with one for each site (fermion occupation) and a register for each link (electric flux). This leaves an exponentially large part of the space unphysical---not satisfying the local constraint of Gauss's Law. Instead, the physical space of desired parity and momentum can be constructed classically with configurations mapped to quantum states. This reduces the simulation of the system above from 12 to 2 qubits.

Statics

Variational Quantum Eigensolver:

The ground state of the Schwinger Model can be initialized and explored through implementation of the variational quantum eigensolver. After decomposing the Hamiltonian in the Pauli basis consisting of the seven operators at right and parameterizing the ground state wavefunction with a 3-angle circuit ansatz, ensemble projective measurements within the four unique bases allow extraction of the angular-dependent Hamiltonian expectation value. Using energy estimates to inform a Bayesian posterior in the 3-dimensional space of angles determines the correct circuit for ground state preparation.

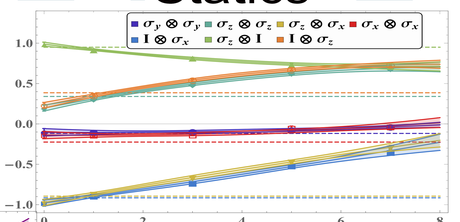

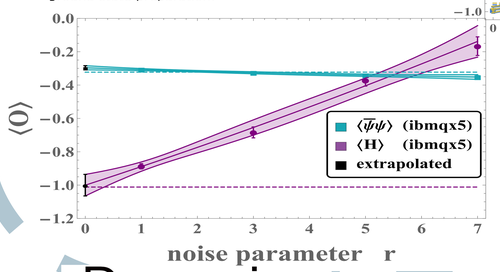

Noise Extrapolation:

Without quantum error correction on hardware with imperfect gates, "classical error correction" (data analysis) is crucial for interpreting and understanding the results of quantum computing experiments. Of critical concern are 2-qubit entanglement errors, measurement/read-out errors, over/under rotations, bit flips, phases errors, etc. We utilize a 1-parameter polynomial extrapolation to capture the leading effects of the first of these. The noise parameter, r, indicates the number of CNOTs used in place of each CNOT of the VQE ansatz (containing only 2 CNOTs in the original, $r = 1$, circuit), effectively amplifying this source of error and allowing its extrapolated removal. As seen at left, this extrapolation impacts the calculated ground state energy at the 10% level.

Dynamics

SU(4) Propagator:

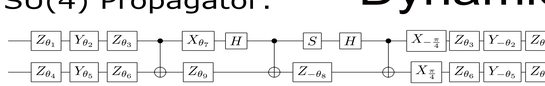

An interesting observable of the Schwinger model is the evolution of electron-positron pair production (as sourced by the Hamiltonian hopping term) following initialization of the empty configuration. At right, we show data and theoretical values for both this pair production and the expectation value of the energy in the electric field. The solid curves are exact results while the data points are quadratic extrapolations (in the noise parameter r) obtained with the ibmqx2 quantum computer. While there is an additional configuration containing two electron-positron pairs whose dynamics are not represented here, the energy in the electric field is seen to correlate naturally with the presence of charged particles. For this calculation, the SU(4) propagator decomposition of [4] is utilized---the nine angles of the above circuit are classically calculated as a function of time. As the structure and depth of the quantum circuit then used to propagate to time t is independent of t, precision of the expectation values is also independent of the scaled time.

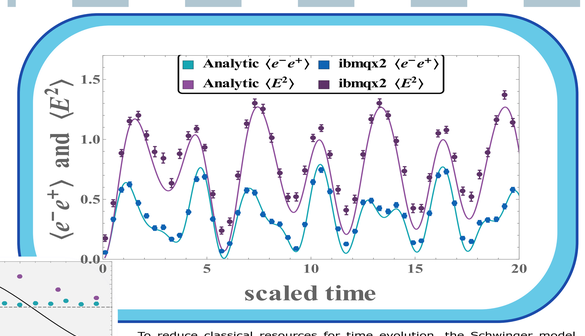

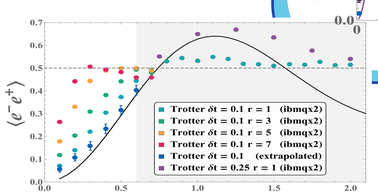

To reduce classical resources for time evolution, the Schwinger model propagator can be decomposed into a sum of 7 Paulis (see statics above) and the exponentials implemented individually, Trotterizing the evolution. Now, rather than fixed as in the SU(4) decomposition method, the required coherence time increases with the scaled time. On the left is the probability of finding an electron-positron pair in the two-spatial-site Schwinger model from the initially-empty state, showing dynamical quantum fluctuations. In the unshaded region, the blue points are quadratic extrapolations to "zero noise" in a parameter, r. For a step size of 0.1, the coherence time is exceeded in the gray region and the measured probabilities flatten to the classical value.

Bibliography: [1] Schwinger, Julian (1962). Gauge Invariance and Mass. II. Phys. Rev., 128, 2425-2429.
[2] Banks, T., Susskind, Leonard & Kogut, John (1976). Strong-coupling calculations of lattice gauge theories: (1 + 1)-dimensional exercises. Phys. Rev. D, 13, 1043-1053.
[3] Coleman, Sidney R. (1976). More About the Massive Schwinger Model. Annals Phys., 101, 239.
[4] G. Vidal and C. M. Dawson, Phys. Rev. A 69, 010301 (2004).
[5] A. Kandala, A. Mezzacapo, K. Temme, M. Takita, M. Brink, J. M. Chow, and J. M. Gambetta, Nature (London) 549, 242 (2017), arXiv:1704.05018 [quant-ph].